Inorg. Chem. **2003**, *42*, 5612–5620

$S = {}^3/_2 \rightleftharpoons S = {}^1/_2$ Spin Crossover Behavior in Five-Coordinate Halido- and Pseudohalido-bis(*o*-iminobenzosemiquinonato)iron(III) Complexes

Hyungphil Chun, Eckhard Bill, Thomas Weyhermüller, and Karl Wieghardt*

Max-Planck-Institut für Bioanorganische Chemie, Stiftstrasse 34-36, D-45470 Mülheim an der Ruhr, Germany

Received May 8, 2003

Five-coordinate halido- and pseudohalido-bis(*o*-iminobenzosemiquinonato)iron(III) complexes $[Fe^{III}X(L^{ISQ})_2]$ (X = Cl^- (**1**), Br^- (**2a**, **2b**), I^- (**3**), N_3^- (**4**), and NCS^- (**5**)) have been synthesized where $(L^{ISQ})^{1\bullet-}$ represents the π radical anion *N*-phenyl-*o*-imino(4,6-di-*tert*-butyl)benzosemiquinonate(1–). The molecular structures of the two polymorphs **2a** and **2b** have been determined at 100, 220, and 295 K, respectively, by single crystal X-ray crystallography. Variable temperature magnetic susceptibility data reveal the following electronic ground states, S_t: For **1**, it is ${}^3/_2$. Polymorph **2a** contains a 1:1 mixture of ${}^3/_2$ and ${}^1/_2$ forms in the range 4.2 to ~150 K; above 150 K the latter form undergoes a spin crossover ${}^1/_2 \rightarrow {}^3/_2$. Polymorph **2b** contains only the $S_t = {}^3/_2$ form (4–300 K). Complex **3** contains the $S_t = {}^1/_2$ form in the range 4–130 K, but above 130 K, a spin crossover to the ${}^3/_2$ form is observed which is confirmed by three crystal structure determinations at 100, 220, and 295 K. Complex **4** possesses an $S_t = {}^1/_2$ ground state at 80 K and undergoes a spin crossover at higher temperatures. Complex **5** has a temperature-independent $S_t = {}^3/_2$ ground state. All crystal structures of **1**, **2a**, **2b**, **3**, **4**, and **5**, regardless at which temperature the data sets have been measured, show that two *o*-iminobenzosemiquinonate(1–) π radical anions are N,O-coordinated in all of these neutral iron complexes. The Fe–N and Fe–O bond distances are longer in the $S_t = {}^3/_2$ and shorter in the $S_t = {}^1/_2$ forms. The $S_t = {}^3/_2$ ground state is attained via intramolecular antiferromagnetic coupling between a high spin ferric ion ($S_{Fe} = {}^5/_2$) and two ligand π radicals whereas the $S_t = {}^1/_2$ form is generated from exchange coupling between an intermediate spin ferric ion ($S_{Fe} = {}^3/_2$) and two ligand radicals.

Introduction

In two recent publications,[1,2] we have described the synthesis and the molecular and electronic structures of iron complexes containing N,O-coordinated *o*-iminobenzosemiquinonate(1−), $(L^{ISQ})^{1\bullet-}$, π radical anions, namely the distorted octahedral species $[Fe^{III}(L^{ISQ})_3]$ and the five-coordinate complexes $[Fe^{III}(L^{ISQ})_2X]$ where X represents Cl^- (**1**), Br^- (**2**), and I (**3**) (Scheme 1). Temperature-dependent magnetic susceptibility measurements revealed that $[Fe^{III}(L^{ISQ})_3]$ has an $S = 1$ ground state which originates from a strong intramolecular antiferromagnetic coupling between a high spin ferric ion (d^5, $S_{Fe} = {}^5/_2$) and three organic π radicals ($S_{rad} = {}^1/_2$). In contrast, **1** has an $S_t = {}^3/_2$, and **3**, an $S_t = {}^1/_2$ ground state, and most interestingly, in **2a** (polymorph 1) two different species with an $S_t = {}^1/_2$ and an $S_t = {}^3/_2$ ground state, respectively, are present in a 1:1 ratio at temperatures < 120 K. The crystal structures determined at 100 K clearly

Scheme 1

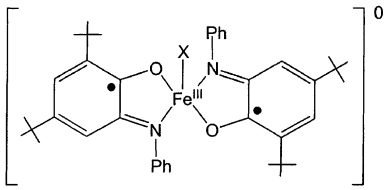

trans - $[Fe^{III}(L^{ISQ})_2Cl]$	$S_t = 3/2$	**1**
trans - $[Fe^{III}(L^{ISQ})_2Br]$	polymorph 1, $S_t = 1/2, 3/2$	**2a**
	polymorph 2, $S_t = 3/2$	**2b**
trans - $[Fe^{III}(L^{ISQ})_2I]$	$S_t = 1/2$	**3**
trans - $[Fe^{III}(L^{ISQ})_2(N_3)]$	$S_t = ½$	**4**
$[Fe^{III}(L^{ISQ})_2(NCS)]$	$S_t = 3/2$	**5**

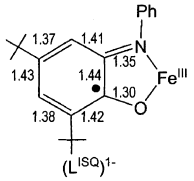

error:
± 0.015 (3σ)

* To whom correspondence should be addressed. E-mail: wieghardt@mpi-muelheim.mpg.de.

(1) Chun, H.; Verani, C. N.; Chaudhuri, P.; Bothe, E.; Bill, E.; Weyhermüller, T.; Wieghardt, K. *Inorg. Chem.* **2001**, *40*, 4157.
(2) Chun, H.; Weyhermüller, T.; Bill, E.; Wieghardt, K. *Angew. Chem., Int. Ed.* **2001**, *40*, 2489.

10.1021/ic0301526 CCC: $25.00
Published on Web 08/14/2003

Table 1. Summary of Bond Distances of Complexes from References 1 and 2 at 100 K and Ground States

complex	av Fe−N, Å[a]	av Fe−O, Å[a]	S_t[b] (S_{Fe})[c]
$[Fe^{III}(L^{ISQ})_3]$	2.099	2.014	1 ($^5/_2$)
1	2.041	1.963	$^3/_2$ ($^5/_2$)
2a	1.892	1.873	$^1/_2$ ($^3/_2$)
	2.047	1.951	$^3/_2$ ($^5/_2$)
3	1.885	1.875	$^1/_2$ ($^3/_2$)

[a] Average Fe−O and Fe−N bond lengths of N,O-coordinated radical anions, $(L^{ISQ})^{1\bullet-}$. [b] Electronic ground state. [c] Local spin state at ferric ion.

show that in these five-coordinate species with an $S_t = {}^3/_2$ ground state a high spin ferric ion and two π radical anions[3] prevail, whereas in the $S_t = {}^1/_2$ species an intermediate spin ferric ion ($S_{Fe} = {}^3/_2$) and two antiferromagnetically coupled ligand radical anions are present. The average Fe−N and Fe−O distances in the $S_t = {}^3/_2$ form are significantly longer than those in the $S_t = {}^1/_2$ form.

It is important to note that in the crystal structures of $[Fe^{III}(L^{ISQ})_3]$, **1**, **2**, and **3** the geometrical features (bond distances and angles) of the N,O-coordinated ligand radical anions are identical within the small experimental errors of high quality, low temperature (100 K) X-ray crystal structure determinations (see Scheme 1). It is only the respective Fe−O and Fe−N distances which clearly vary as a function of the local spin state of the respective iron ion as summarized in Table 1. The local spin states of the ferric ions were most clearly established by Mössbauer spectroscopy where species with a local $S_{Fe} = {}^5/_2$ configuration like **1** and **2b** display an isomer shift at 80 K of ~0.46 mm s^{-1} or 0.54 mm s^{-1} for $[Fe(L^{ISQ})_3]$, whereas those with an intermediate spin ferric ion, $S_{Fe} = {}^3/_2$, have values for δ of ~0.24 mm s^{-1}.

In an attempt to reproduce our previous results[2] for **2a**, we have now discovered that a second polymorph 2 (**2b**) can be isolated which contains exclusively neutral molecules $[FeBr(L^{ISQ})_2]$ with an $S_t = {}^3/_2$ ground state. In addition, we synthesized $[Fe(N_3)(L^{ISQ})_2]$ (**4**) which has an $S_t = {}^1/_2$ and $[Fe(NCS)(L^{ISQ})_2]$ (**5**) with an $S_t = {}^3/_2$ ground state. Temperature-dependent X-ray crystallography of **2a**, **2b**, **3**, and **4** in conjunction with variable temperature susceptibility measurements and Mössbauer spectroscopy show unambiguously that spin crossover behavior $S_t = {}^3/_2 \leftrightharpoons S_t = {}^1/_2$ exists in these complexes.

Experimental Section

The ligand 2-anilino-4,6-di-*tert*-butylphenol, $H[L^{AP}]$,[4,5] and complexes **1**, **2a** (polymorph 1), and **3** have been prepared as described in the literature.[2,4]

***trans*-$[Fe^{III}(L^{ISQ})_2Br]$ (2b) (Polymorph 2).** To a solution of $FeBr_2$ (0.33 g; 1.5 mmol) in 40 mL of distilled methanol was added a methanolic solution (20 mL) of the ligand $H_2(L^{AP})$ (0.45 g; 1.5 mmol) and $NaOCH_3$ (0.16 g; 3 mmol). The filtered solution was stirred at 20 °C in the presence of air for 1 h and allowed to stand for a few hours in an open vessel whereupon a brown-black microcrystalline precipitate formed which was collected by filtration. Yield: 0.37 g. Anal. Calcd for $C_{40}H_{50}N_2O_2BrFe$: C, 66.12; H, 6.94; N, 3.86; Br, 11.00. Found: C, 65.9; H, 7.1; N, 3.8; Br, 10.9.

***trans*-$[Fe^{III}(L^{ISQ})_2(N_3)]$ (4).** To a dark red methanol solution (20 mL) of $[Fe^{III}(dmf)_6](ClO_4)_3$ (dmf = dimethylformamide) (0.40 g; 0.5 mmol) and NaN_3 (0.13 g; 2 mmol) was added at 20 °C the ligand in two separate portions of 0.20 g (0.7 mmol), and after 30 min of stirring in the presence of air, another 0.06 g (0.2 mmol) of $H[L^{AP}]$ was added. The resulting slurry was allowed to stand overnight and was then filtered to collect a microcrystalline dark precipitate. Yield: 0.24 (80%). Single crystals suitable for X-ray crystallography were obtained by slow evaporation of an $CH_3CN/CHCl_3$ (1:1) solution of **4** under an Ar atmosphere. Anal. Calcd for $C_{40}H_{50}N_5O_2Fe$ (fw 689): C, 69.72; H, 7.32; N, 10.16. Found: C, 69.6; H, 7.1; N, 10.0. EI-mass spectrum: $m/z = 688$ $\{M\}^+$, 646 $\{M - N_3\}^+$ 100%. IR($CHCl_3$): $\nu_{as}(N_3)$ 2061 cm^{-1}. KBr disk: $\nu_{as}(N_3)$ 2057, 2035, 2005 cm^{-1}.

***trans*-$[Fe^{III}(L^{ISQ})_2(NCS)]$ (5).** $[Fe(dmf)_6](ClO_4)_3$ (0.40 g; 0.5 mmol) was added to a methanol solution (25 mL) of K[SCN] (0.20 g; 2.0 mmol) yielding a dark reddish purple solution to which the ligand $H[L^{AP}]$ (0.20 g; 0.7 mmol) was added in two portions with a 30 min interval. After 1 h of stirring in the presence of air, $H[L^{AP}]$ (0.10 g; 0.3 mmol) was added to the solution which was stirred for another hour. The resulting solution was filtered, and triethylamine (0.10 mL) was added. After stirring at 20 °C for 3 h whereupon a color change to dark green was observed, a dark precipitate formed which was collected by filtration. Yield: 0.20 g (56%). Anal. Calcd for $C_{41}H_{50}N_3O_2SFe$ (fw 704.8): C, 69.87; H, 7.15; N, 5.96. Found: C, 69.7; H, 7.0; N, 6.0. EI-mass spectrum: $m/z = 704$ $\{M\}^+$, 646 $\{M - NCS\}^+$. IR(KBr disk): ν(NCS) 2050 cm^{-1}. Recrystallization from a saturated $CHCl_3$ solution yielded single crystals of **5**·$CHCl_3$ suitable for X-ray crystallography.

Physical Measurements. Electronic spectra of complexes were recorded with an HP 8452A diode array spectrophotometer (range: 190−1100 nm). Variable temperature (3−298 K) magnetization data were measured using a SQUID magnetometer (MPMS Quantum design) in an external magnetic field of 1.0 T. The experimental susceptibility data were corrected for underlying diamagnetism by use of tabulated Pascal's constants. The X-band EPR spectrum was recorded on a Bruker ESP 300 spectrometer. The ^{57}Fe, zero-field Mössbauer spectra were measured on an Oxford Instruments Mössbauer spectrometer. ^{57}Co/Rh was used as radiation source. The temperature of the sample was controlled by an Oxford Instruments Variox cryostat. Isomer shifts were determined relative to α-iron at 300 K. The minimum experimental line width was 0.24 mm s^{-1}.

X-ray Crystallography. Black single crystals of **2a**, **2b**, **3**, and **4**, respectively, were coated with perfluoropolyether, picked up with glass fibers, and mounted on a Nonius Kappa-CCD diffractometer equipped with a nitrogen cryostream setup. Intensity data were collected using the same respective single crystal at temperatures between 100 and 295 K using graphite monochromated Mo Kα radiation ($\lambda = 0.71073$ Å) of a rotating anode source. Final cell constants were obtained from a least-squares fit of a subset of several thousand strong reflections. Data collection was performed by full-sphere runs taking frames at 1.0° in ω . Crystal faces were determined, and the Gaussian type empirical absorption correction embedded in XPREP[6a] was used to correct for absorption. The ShelXTL[6a] software package was used for solution and artwork of the structure which was readily solved by Patterson methods and difference Fourier techniques, and ShelXL-97[6b] was used for structure refinement. All non-hydrogen atoms were refined aniso-

(3) Sun, X.; Chun, H.; Hildenbrand, K.; Bothe, E.; Weyhermüller, T.; Neese, F.; Wieghardt, K. *Inorg. Chem.* **2002**, *41*, 4295.
(4) Chaudhuri, P.; Verani, C. N.; Bill, E.; Bothe, E.; Weyhermüller, T.; Wieghardt, K. *J. Am. Chem. Soc.* **2001**, *123*, 2213.
(5) (a) Maslovskaya, L. A.; Petrikevich, D. K.; Timoshchuk, V. A.; Shadyro, O. I. *Russ. J. Gen. Chem. (Engl. Transl.)* **1996**, *66*, 1842; *Zh. Obshch. Khim.* **1996**, *66*, 1893.

Table 2. Crystallographic Data for **2a**, **2b**, **3**, **4**, and **5**

	2a			**2b**		**3**		**4**		**5**·$CHCl_3$
temp, K	220	295	100	200	295	220	295	100	295	100(2)
chem formula	$C_{40}H_{50}BrFeN_2O_2$			$C_{40}H_{50}BrFeN_2O_2$		$C_{40}H_{50}FeIN_2O_2$		$C_{40}H_{50}FeN_5O_2$		$C_{42}H_{51}Cl_3N_3O_2SFe$
cryst size, mm^3	$0.20 \times 0.20 \times 0.05$			$0.68 \times 0.43 \times 0.17$		$0.30 \times 0.20 \times 0.14$		$0.33 \times 0.33 \times 0.28$		$0.08 \times 0.13 \times 0.17$
fw	726.58			726.58		773.57		688.70		842.12
space group	$P\bar{1}$, No. 2			$P\bar{1}$, No. 2		$P2_1/c$, No. 14		$P2_1$, No. 4		$P2_1/n$, No. 14
a, Å	10.6008(3)	10.6911(3)	10.7103(8)	10.8033(8)	10.8656(6)	13.5473(4)	13.6151(9)	13.2976(5)	13.2961(4)	10.2261(4)
b, Å	14.8013(6)	14.8140(6)	13.1952(8)	13.2566(8)	13.2698(6)	26.4964(8)	26.707(2)	10.9599(4)	11.1489(4)	20.3776(12)
c, Å	24.5204(12)	24.5487(9)	14.0230(10)	14.1489(12)	14.2306(8)	11.7437(4)	11.7923(9)	13.9542(5)	14.1492(4)	21.8055(12)
α, deg	86.62(1)	86.37(1)	74.77(1)	74.95(1)	75.13(2)	90		90		90
β, deg	85.06(1)	85.48(1)	79.79(1)	79.60(1)	79.53(2)	112.87(1)	112.68(1)	112.72(1)	112.94(1)	91.86(1)
γ, deg	87.53(1)	87.50(1)	76.51(1)	77.47(1)	77.94(2)	90		90		90
V, $Å^3$	3823.6(3)	3865.2(2)	1845.2(2)	1893.6(2)	1921.5(2)	3884.1(2)	3956.3(5)	1875.88(12)	1931.55(11)	4541.5(4)
Z	4			2		4		2		4
ρ calcd, g cm^{-3}	1.262	1.249	1.308	1.274	1.256	1.323	1.299	1.219	1.184	1.205
reflns collected/ $2\theta_{max}$[a]	63445/50.00	78537/48.28	18351/61.98	21162/60.00	19318/60.00	100548/61.96	26289/61.04	45229/66.36	51050/61.98	68121/50.0
unique reflns/ $I > 2\sigma(I)$	13430/9680	12261/9463	11575/10261	10672/8550	10983/8289	12353/10182	11081/6801	14290/13603	12239/10023	7789
no. params	829			415		427		445		491
μ(Mo Kα), cm^{-1}	14.74	14.58	15.27	14.88	14.66	12.17	11.95	4.42	4.29	5.90
R1[b]/GOF[c]	0.0462/1.011	0.0490/1.042	0.0424/1.039	0.0509/1.043	0.0479/1.010	0.0299/1.030	0.0488/1.020	0.0337/1.047	0.0355/1.010	0.096/1.238
wR2[d] ($I > 2\sigma(I)$)	0.0931	0.1076	0.1034	0.1333	0.1162	0.0662	0.0924	0.0850	0.0858	0.2167

[a] Diffractometer used in all cases: Nonius Kappa-CCD. [b] $I > 2\sigma(I)$. $R1 = \sum||F_o| - |F_c||/\sum|F_o|$. [c] $GOF = [\sum[w(F_o^2 - F_c^2)^2]/(n - p)]^{1/2}$. [d] $wR2 = [\sum[w(F_o^2 - F_c^2)^2]/\sum[w(F_o^2)^2]]^{1/2}$ where $w = 1/\sigma^2(F_o^2) + (aP)^2 + bP$, $P = (F_o^2 + 2F_c^2)/3$.

tropically, and hydrogen atoms were placed at calculated positions and refined as riding atoms with isotropic displacement parameters. The absolute structure parameter for complex **4** was reliably determined. Crystallographic data of the compounds and diffractometer types used are listed in Table 2.

Results and Discussion

1. Syntheses. It has previously been shown that the reaction of the ligand 2-anilino-4,6-di-*tert*-butylphenol, H[L^{AP}], in methanol or ethanol/dichloromethane (1:1 vol) with $FeCl_2 \cdot 4H_2O$, $FeBr_2$, or FeI_2 dissolved in methanol yields in the presence of oxygen dark neutral molecules of [$Fe^{III}(L^{ISQ})_2$-Cl] (**1**), [$Fe^{III}(L^{ISQ})_2Br$] (**2a**), and [$Fe^{III}(L^{ISQ})_2I$] (**3**).[2] $(L^{ISQ})^{1\bullet-}$ represents the *o*-iminobenzosemiquinonate(1−) π radical anion. Complex **2a** has been synthesized in the presence of 2 equiv (relative to $FeBr_2$) of triphenylphosphine, PPh_3, which was used as a reagent to facilitate crystallization and the growth of single crystals suitable for X-ray crystallography.

We have now discovered that the reaction described here for the preparation of **2a** yields in the *absence* of PPh_3 a second polymorph of [$Fe^{III}(L^{ISQ})_2Br$] (**2b**). The two polymorphs **2a** and **2b** differ most significantly in the temperature dependence of their magnetic susceptibilities ($\chi_M \cdot T$ vs T curves) as is shown in Figure 1. We have also determined the crystal structure of **2b**; that of **2a** has been reported in ref 2. Both polymorphs crystallize in the triclinic space group $P\bar{1}$ but with $Z = 4$ for **2a** and $Z = 2$ for **2b**. The spectroscopic and magnetic consequences of this difference will be discussed in detail in the following.

[$Fe^{III}(dmf)_6$](ClO_4)$_3$ (dmf = dimethylformamide) in CH_3OH reacted with the ligand H[L^{AP}] in the presence of NaN_3 or K[SCN] and dioxygen. After the addition of $N(Et)_3$, dark precipitates of [$Fe^{III}(L^{ISQ})_2(N_3)$] (**4**) and [$Fe(L^{ISQ})_2$(NCS)] (**5**) formed within a few hours. In the infrared spectrum of **4** (KBr disk), three $\nu(N_3)$ stretching frequencies were observed at 2057(w), 2035(m), and 2005(s) cm^{-1}, but in chloroform solution only a single band at 2061 cm^{-1} was observed. The IR spectrum of **5** displays a ν(NCS) stretching frequency at 2050 cm^{-1} which is typical for N-coordinated thiocyanato ligands.[7] It is surprising that **4** possesses an $S_t = {}^1/_2$ ground state whereas **5** has an $S_t = {}^3/_2$ ground state.

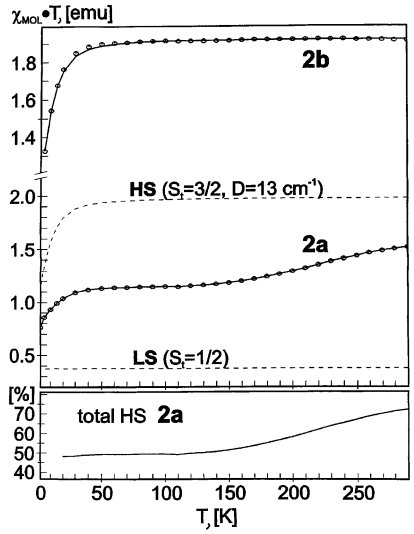

Figure 1. Plot of $\chi_M \cdot T$ vs T for solid samples of **2a** and **2b** (top) and temperature dependence of the amount of the high spin component in **2a** (bottom). The dotted lines (· · ·) represent calculated curves for a 100% high spin component with $S_t = {}^3/_2$ and $|D_{3/2}| = 13$ cm^{-1} and 100% low spin component with $S_t = {}^1/_2$.

The electronic spectra of complexes **1**, **2a**, **3**, **4**, and **5** in CH_2Cl_2 are shown in Figure 2 (Table 3); they are similar

(6) (a) *ShelXTL V.5*; Siemens Analytical X-ray Instruments, Inc.: Madison, WI, 1994. (b) Sheldrick, G. M. *ShelXL-97*; Universität Göttingen: Göttingen, Germany, 1997.

(7) Nakamoto, K. *Infrared and Raman Spectra of Inorganic and Coordination Compounds*, 5th ed.; Wiley: New York; Part B, p 116.

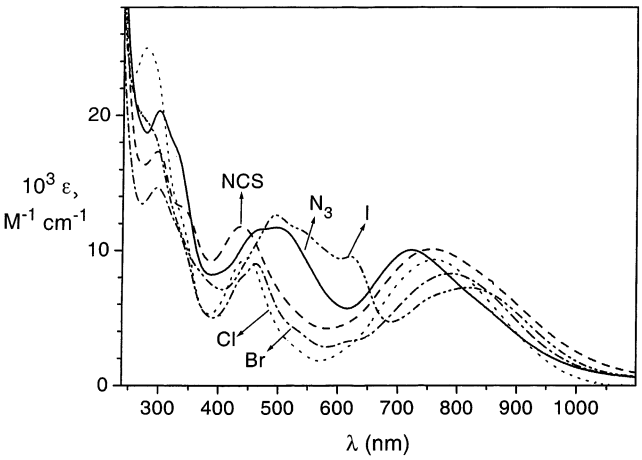

Figure 2. Electronic spectra of complexes **1**, **2a**, **3**, **4**, and **5** in CH_2Cl_2 solution at 20 °C.

Table 3. Electronic Spectra of Complexes in CH_2Cl_2 Solution

complex	λ_{max}, nm (ϵ, L mol^{-1} cm^{-1})
1	290 (2.5×10^4), 350sh (1.3×10^4), 455 (0.95×10^4), 760 (0.93×10^4)
2	300sh (1.4×10^4), 460 (0.8×10^4), 800 (0.8×10^4)
3	305 (1.7×10^4), 480 (1.3×10^4), 550sh, 640 (0.95×10^4), 840 (0.6×10^4)
4	299 (2.0×10^4), 330sh (1.7×10^4), 469 (1.2×10^4), 497 (1.2×10^4), 720 (1.0×10^4)
5	296 (1.7×10^4), 340sh (1.3×10^4), 437 (1.2×10^4), 755 (1.0×10^4)

and exhibit a very intense absorption maximum in the range 700−850 nm ($\epsilon \sim 0.8-1.0 \times 10^4$ L mol^{-1} cm^{-1}) and another in the range 400−500 nm ($\epsilon \sim 0.9-1.2 \times 10^4$ L mol^{-1} cm^{-1}).

2. Magnetic Properties of Complexes. Variable temperature (3−300 K) measurements of the magnetic susceptibility of complexes **1** and **3** have been reported previously.[2] Complex **1** possesses a temperature-independent effective magnetic moment of 3.91 μ_B in the range 60−300 K indicating an $S_t = {}^3/_2$ ground state for [$Fe^{III}(L^{ISQ})_2Cl$] (**1**). Below 60 K, the magnetic moment drops to 2.8 μ_B at 3 K. This temperature dependence was successfully accounted for by introducing a zero-field parameter $|D_{3/2}|$ of 18 cm^{-1}.

In contrast, the temperature independence of the effective magnetic moment of **3** in the range 5−150 K of 1.9 μ_B is compatible only with an $S_t = {}^1/_2$ ground state for [$Fe^{III}(L^{ISQ})_2I$] (**3**), but above 150 K, μ_{eff} increases monotonically to 2.7 μ_B per Fe^{III} at 300 K as shown in Figure 3. This behavior had been successfully modeled[2] by assuming intramolecular exchange coupling between two π radical ligands, $S_{rad} = {}^1/_2$, and a central intermediate spin ferric ion ($S_{Fe} = {}^3/_2$). By using the Hamiltonian $H = -2JS_{rad}\cdot S_{Fe}$ ($S_{rad} = {}^1/_2$, $S_{Fe} = {}^3/_2$), a strong intramolecular antiferromagnetic coupling of $J = -145(20)$ cm^{-1} would be typical for such complexes. Since we have recorded[2] the Mössbauer spectrum of **3** at 80 and 298 K (Table 4) and observed only a single quadrupole doublet in both cases, we thought at the time that we can rule out the alternative model which would invoke a spin crossover $S_t = {}^1/_2 \rightleftharpoons S_t = {}^3/_2$ of **3**. As we will show here, the Fe−N and Fe−O bond lengths in **3** increase with increasing temperature. This can only be due to

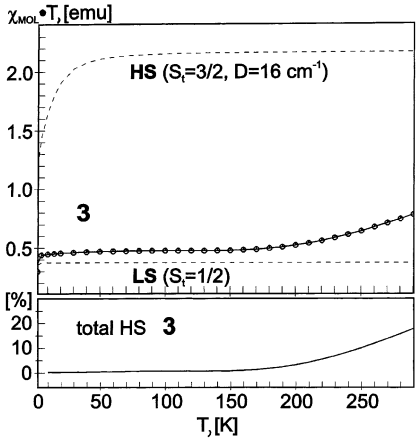

Figure 3. Top: Plot of $\chi_M \cdot T$ vs T for a solid sample of [$Fe^{III}(L^{ISQ})_2I$] (**3**). Open circles (○) are experimental values, and the solid line (−) is a best fit. Broken lines (- - -) represent curves for a 100% high spin component ($S_t = {}^3/_2$, $g = 2.1$, and $|D_{3/2}| = 16$ cm^{-1}) and 100% low spin component ($S_t = {}^1/_2$, $g = 2.16$). Bottom: Percentage of total high spin [$Fe^{III}(L^{ISQ})_2I$] form as a function of the temperature.

Table 4. Zero-Field Mössbauer Parameters of Complexes

complex	T, K	S_t[a]	isomer shift, δ, mm s^{-1}	quadrupole splitting, ΔE_Q, mm s^{-1}
1	80	${}^3/_2$	0.45	1.26
2a	80	${}^3/_2$	0.47	1.22
	80	${}^1/_2$	0.23	2.62
2b	80	${}^3/_2$	0.47	1.33
3	80	${}^1/_2$	0.24	2.80
	298	${}^1/_2 \rightleftharpoons {}^3/_2$	0.22	2.21
4	80	${}^1/_2$	0.20	2.42
5	80	${}^3/_2$	0.43	1.26
2a	150	${}^3/_2$	0.45	1.23
		${}^1/_2 \rightleftharpoons {}^3/_2$	0.22	2.54
	200	${}^3/_2$	0.43	1.22
		${}^1/_2 \rightleftharpoons {}^3/_2$	0.25	2.17
	250	${}^3/_2$	0.39	1.20
		${}^1/_2 \rightleftharpoons {}^3/_2$	0.27	1.73
	295	${}^3/_2$, ${}^1/_2 \rightleftharpoons {}^3/_2$	0.32	1.30
2b	130	${}^3/_2$	0.45	1.32
	295	${}^3/_2$	0.36	1.17

[a] Spin state of [$Fe^{III}X(L^{ISQ})_2$] molecules.

temperature-dependent spin crossover behavior $S_t = {}^1/_2 \rightarrow S_t = {}^3/_2$. At 295 K, the observed effective magnetic moment of 2.7 μ_B is then due to the presence of 37% of the $S_t = {}^3/_2$ and 63% of the $S_t = {}^1/_2$ forms. These values agree nicely with the crystallographic analysis using the Fe−O and Fe−N bond lengths of the pure $S_t = {}^3/_2$ and ${}^1/_2$ forms (see following paragraphs).

Figure 1 exhibits the plot of $\chi_M \cdot T$ vs T of solid samples of **2a** and **2b**, the two polymorphs of [$Fe^{III}(L^{ISQ})_2Br$]. Surprisingly, the two curves differ significantly despite the fact that both polymorphs contain only neutral molecules of [$Fe^{III}(L^{ISQ})_2Br$]. The μ_{eff}/Fe value of crystals of **2a** is nearly temperature independent at 3.08 μ_B in the range 50−140 K; it then increases to 3.56 μ_B at 295 K, and it decreases in the range 50−3 K from 3.08 to 2.48 μ_B. This behavior is perfectly modeled assuming a 1:1 mixture of an $S_t = {}^3/_2$ and an $S_t = {}^1/_2$ species in the range 50−140 K as indicated by the crystal structure at 100 K.[2] The decrease of μ_{eff} in the range 50−3 K is due to zero-field splitting of $|D_{3/2}| = 18$ cm^{-1} of the $S_t = {}^3/_2$ species, and the increase of μ_{eff} above 140 K is due to spin crossover $S_t = {}^1/_2 \rightarrow S_t = {}^3/_2$ behavior

of the one-half of the $[Fe(L^{ISQ})_2Br]$ molecules possessing an $S_t = {}^1/_2$ ground state below 140 K. From the crystal structure at 295 K (see following description), we calculate a ratio of 81.5% of the $S_t = {}^3/_2$ form and 18.5% of the $S_t = {}^1/_2$ form to be present which according to the relation μ_{eff} (295 K) = $[0.185(1.73)^2 + 0.815(3.87)^2]^{1/2}$ yields an effective magnetic moment of 3.57 μ_B at 295 K which agrees well with the observed value of 3.6 μ_B.

On the other hand, **2b** displays a temperature-independent magnetic moment of 3.9 μ_B in the range 50−300 K. Below 50 K, a decrease to 3.26 μ_B at 3 K is due to zero-field splitting $|D_{3/2}| = 18$ cm^{-1}. Thus, in agreement with the crystal structure determinations at 100, 200, and 300 K (see following descriptions), **2b** consists of $[Fe^{III}(L^{ISQ})_2Br]$ $S_t = {}^3/_2$ molecules only.

The effective magnetic moment of **4** in the range 50−150 K of 1.9 μ_B is indicative of the presence of an $S_t = {}^1/_2$ species. At temperatures > 150 K, μ_{eff} increases slowly to 2.7 μ_B at 300 K which indicates again an $S_t = {}^1/_2 \rightarrow S_t = {}^3/_2$ crossover as in **3**. Interestingly, **5** contains only the $S_t = {}^3/_2$ form $\mu_{eff} \sim 3.9$ μ_B in the range 60−300 K.

3. Mössbauer Spectroscopy. The zero-field Mössbauer spectra of **1**, **2a**, and **3** have been recorded previously; the isomer shift and quadrupole splitting parameters at 80 K are summarized in Table 4. We also recorded the spectra of **4** and **5** at 80 K which both display a single quadrupole doublet.

The Mössbauer parameters clearly allow us to distinguish between species with $S_t = {}^3/_2$ and those possessing an $S_t = {}^1/_2$ ground state. The former complexes have isomer shifts in the narrow range 0.43−0.47 mm s^{-1} at 80 K and quadrupole splittings $|\Delta E_Q|$ of 1.22−1.33 mm s^{-1} indicating the presence of high spin ferric ions ($S_{Fe} = {}^5/_2$), whereas the latter have δ values of 0.22 mm s^{-1} and large quadrupole splittings of 2.37−2.80 mm s^{-1} indicative of intermediate spin ferric ions ($S_{Fe} = {}^3/_2$).[8] The azido species **4** consists exclusively of the $S_t = {}^1/_2$ form at 80 K whereas the N-coordinated thiocyanato species **5** possesses the Mössbauer parameters typical of the $S_t = {}^3/_2$ form.

It is interesting to note that the Mössbauer spectrum of **2a** containing an $S_t = {}^3/_2$ and a ${}^1/_2$ species in a 1:1 ratio <120 K displays two quadrupole doublets at 80 K whereas for **2b**, only a single quadrupole doublet has been observed. These data are shown in Figure 4 for **2a** and Figure 5 for **2b** together with their respective temperature dependence. That of the isomer shift and quadrupole splitting parameter for **2b** containing only $S_t = {}^3/_2$ species in the range 80−300 K is typical for a single high spin ferric ion ($S_{Fe} = {}^5/_2$). The isomer shift, δ, decreases from 0.47 mm s^{-1} at 80 K to 0.36 mm s^{-1} at 300 K, and the quadrupole splitting, ΔE_Q, is nearly temperature independent in the same range (1.33−1.16 mm s^{-1}).

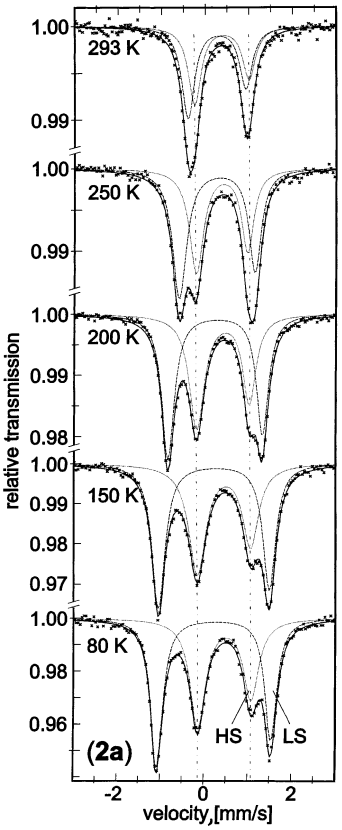

Figure 4. Zero-field Mössbauer spectra of **2a** as a function of the temperature (see Table 4 for data).

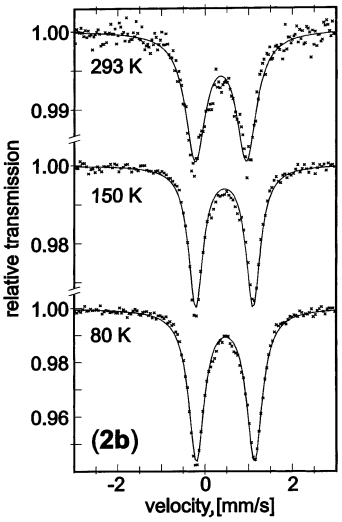

Figure 5. Zero-field Mössbauer spectra of **2b** as a function of the temperature (see Table 4 for data).

The subspectrum of the $S_t = {}^1/_2$ species in **2a** (labeled LS in Figure 4) shows a remarkable temperature dependence which is not consistent with the usual thermal behavior of the electronic structure parameters. In particular, the isomer shift shows an increase from 0.23 mm s^{-1} at 80 K to 0.27 mm s^{-1} at 250 K, in contrast to the expected decrease of up to 0.1 mm s^{-1} caused by second-order-Doppler shift (SOD)

(8) See for example: (a) Koch, S.; Holm, R. H.; Frankel, R. B. *J. Am. Chem. Soc.* **1975**, *97*, 6714. (b) Riley, D. P.; Busch, D. H. *Inorg. Chem.* **1984**, *23*, 3235. (c) Kostka, K. L.; Fox, B. G.; Hendrich, M. P.; Collins, T. J.; Rickard, C. E. F.; Wright, L. J.; Münck, E. *J. Am. Chem. Soc.* **1993**, *115*, 6746. (d) Keutel, H.; Käpplinger, I.; Jäger, E.-G.; Grodzicki, M.; Schünemann, V.; Trautwein, A. X. *Inorg. Chem.* **1999**, *38*, 2320. (e) Jäger, E.-G.; Keutel, H. *Inorg. Chem.* **1997**, *36*, 3512. (f) Nicarchos, D.; Kostikas, A.; Simopoulos, D.; Coucouvanis, D.; Piltingsrud, D.; Coffman, R. E. *J. Chem. Phys.* **1978**, *69*, 4411.

and thermal bond expansions. Also, the variation of the quadrupole splitting from 2.62 mm s^{-1} at 80 K to 1.73 mm s^{-1} at 250 K exceeds the possible range of changes in the electric field gradient (efg) potentially caused by thermal population of different spin−orbital states, particularly since there is no variation of ΔE_Q below 80 K. Such changes strongly indicate transitions to another electronic structure, which is in this case the high spin state of the central iron. Apparently, the ^{57}Fe Mössbauer nucleii of these "low spin" sites in the crystal structure of **2a** experience flips of their local electronic surrounding between $S_{Fe} = {}^3/_2$ ($S_t = {}^1/_2$) and $S_{Fe} = {}^5/_2$ ($S_t = {}^3/_2$), with increasing dwell time on $S_{Fe} = {}^5/_2$ at higher temperatures. The transition rate is apparently fast compared to the time average lifetime of the nucleus ($\approx 10^{-7}$ s, or their quadrupole precession time). Therefore, at any temperature only a single quadrupole spectrum is observed for the species "LS" with isomer shift and quadrupole splittings that are the weighted average of the limiting cases for $S_{Fe} = {}^3/_2$ ($S_t = {}^1/_2$) and $S_{Fe} = {}^5/_2$ ($S_t = {}^3/_2$) (see Table 4 for comparison values). The weight factors could be taken from the abundance of the high-spin species derived from the deconvolution of susceptibility data shown as "total HS" at the bottom of Figure 1. The peculiar increase of the isomer shift and decrease of the quadrupole splitting originate from the higher isomer shift and lower quadrupole splitting of the $S_{Fe} = {}^5/_2$ ($S_t = {}^3/_2$) high temperature state with respect to the $S_{Fe} = {}^3/_2$ ($S_t = {}^1/_2$) low temperature species, and the gradual change reflects the gradual transition of each of these iron sites in the time average.

In contrast, the permanent high spin species in **2a**, which occupies another crystal site and shows an independent Mössbauer subspectrum (HS), is persistently present over the whole temperature range investigated (80−300 K), like the persistent $S_t = {}^3/_2$ state of **2b**.

These temperature dependencies allow us to rationalize the previous observation[2] that **3** displays at 295 K a single asymmetric quadrupole doublet despite the fact that crystallography shows (see the following subsection) that at this temperature the [$Fe^{III}I(L^{ISQ})_2$] molecules exist in their $S_t = {}^3/_2$ and ${}^1/_2$ forms in a ratio 16:84. In other words, one might have expected to observe two doublets. As shown in Table 4 and Figure 4 for [$Fe^{III}Br(L^{ISQ})_2$], the quadrupole splitting parameter and the isomer shift values of the $S_t = {}^3/_2$ and ${}^1/_2$ form become rather similar at 293 K, and one unresolved, asymmetric quadrupole doublet results.

In a recent paper,[9] we have reported the variable magnetic field Mössbauer spectra of [$Fe^{III}I(L^{ISQ})_2$] (**3**) at 4.2 K. From the deduced intrinsic hyperfine coupling constant **A** values of $\mathbf{A}(S_{Fe} = {}^3/_2)/g_N\beta_N = (-12.4, -20.3, +1.3)$ T of the iron(III) ion, it was concluded that the ferric ion possesses a local intermediate spin configuration ($S_{Fe} = {}^3/_2$) like Collins' complex L′Fe^{III}Cl in ref 7c. This intermediate spin ferric ion couples intramolecularly with two *o*-iminobenzosemiquinonate π radicals in an antiferromagnetic fashion yielding the observed $S_t = {}^1/_2$ ground state.

(9) Ghosh, P.; Bill, E.; Weyhermüller, T.; Wieghardt, K. *J. Am. Chem. Soc.* **2003**, *125*, 3967.

4. Crystal Structures. The crystal structures of **1**, **2a**, and **3** have been determined at 100 K previously.[2] The most salient features of this crystallographic work are the following observations. (i) All three crystals consist of neutral pentacoordinate molecules with a square base pyramidal FeN_2O_2X coordination polyhedron where the ligand X (Cl^- in **1**, Br^- in **2a**, and I^- in **3**) occupies the respective apical position and two O,N-coordinated *o*-iminobenzosemiquinonate(1−) π radicals are bound in the basal positions (in *trans*-position with respect to each other). (ii) It is of importance to note that the geometrical details of the O,N-coordinated $(L^{ISQ})^{1-}$ π radicals are identical in all three structures within our small 3σ limit of ±0.01 Å; the average C−O, C−N, and C−C bond lengths are as summarized in Scheme 1. (iii) As pointed out previously,[2] the average Fe−O and Fe−N distances in **1** ($S_t = {}^3/_2$) are comparatively long at 1.963(1) and 2.042(2) Å, respectively, but significantly shorter in **3** ($S_t = {}^1/_2$) at 1.875(1) and 1.885(2) Å, respectively. This large difference of bond lengths is due to the fact that **1** contains a ferric ion with a local high spin configuration ($S_{Fe} = {}^5/_2$) but in **3** an intermediate spin ferric ion ($S_{Fe} = {}^3/_2$) is present. Thus, the antibonding $d_{x^2-y^2}$ orbital is half occupied in **1** but empty in **3**. Consequently, the difference between the average Fe−O and Fe−N bond lengths in $S_t = {}^3/_2$ and $S_t = {}^1/_2$ species is large: Δ(Fe−N) = 0.156 Å, Δ(Fe−O) = 0.083 Å. (iv) In the unit cell of **2a**, there are four neutral molecules of [$Fe^{III}(L^{ISQ})_2Br$]. Since the space group is $P\bar{1}$, there are two crystallographically independent molecules present in the unit cell at sites 1 and 2, respectively. The Fe−N and Fe−O distances of those molecules residing on site 1 are long indicating the presence of the $S_t = {}^3/_2$ form whereas those on site 2 are comparatively shorter and belong to the $S_t = {}^1/_2$ form. (v) Interestingly, the difference Δ(Fe−Br) in **2a** between the $S_t = {}^3/_2$ and the ${}^1/_2$ form is within experimental error, negligible at 0.003 ± 0.003 Å. This is rationalized by the fact that in both forms the d_{z^2} metal orbital is occupied by one electron.

We have now collected data sets of the same crystal of **2a** which has been used for the 100 K determination at 220 and at 295 K and determined the structures again. The results are summarized in Table 5; Figure 6 shows a neutral [Fe(L^{ISQ})$_2$Br] ($S_t = {}^3/_2$) molecule in **2b**. The space group $P\bar{1}$ with $Z = 4$ of **2a** does not change in the temperature range 100−300 K; no phase transition is observed. It is significant that the Fe−Br, Fe−O, and Fe−N bond distances of those molecules residing on site 1 ($S_t = {}^3/_2$) do not vary with temperature as shown in Table 5 and Figure 7. In contrast, those of molecules residing on site 2 with $S_t = {}^1/_2$ at 80 K do vary significantly: they apparently increase with increasing temperature.

Since the Fe−N and Fe−O bond lengths of the pure $S_t = {}^3/_2$ and $S_t = {}^1/_2$ forms are known from **1** and **3** and since these distances do not vary with temperature, it is possible to determine the percentage of the two forms distributed over site 2 in **2a** as shown in Figure 8. It is established that, at 220 K, ∼30% of the molecules on site 2 possess a ${}^3/_2$ ground state and 70% are in the $S_t = {}^1/_2$ form; at 295 K this ratio is

Table 5. Selected Bond Distances (Å) in the Two Polymorphs (**2a**, **2b**) as a Function of the Temperature[a]

	polymorph **2a**[b]						polymorph **2b**		
	100 K		220 K		295 K		100 K	200 K	295 K
	site 2	site 1	site 2	site 1	site 2	site 1			
Br−Fe	2.3665(9)	2.3694(9)	2.3633(6)	2.3716(6)	2.357(1)	2.366(1)	2.3708(3)	2.3686(5)	2.3606(5)
O2−Fe	1.877(3)	1.953(3)	1.908(2)	1.958(2)	1.925(3)	1.947(2)	1.955(1)	1.958(2)	1.957(2)
O1−Fe	1.869(3)	1.950(3)	1.902(2)	1.949(2)	1.926(3)	1.952(2)	1.962(1)	1.960(2)	1.957(2)
N2−Fe	1.886(4)	2.045(4)	1.932(3)	2.046(3)	1.976(4)	2.041(3)	2.045(2)	2.044(2)	2.038(2)
N1−Fe	1.897(4)	2.050(4)	1.939(3)	2.040(3)	1.981(4)	2.043(3)	2.046(2)	2.045(2)	2.041(2)
O1−C1	1.306(5)	1.297(5)	1.307(4)	1.299(4)	1.299(4)	1.288(4)	1.297(2)	1.294(3)	1.290(2)
O2−C21	1.310(5)	1.285(5)	1.300(4)	1.292(4)	1.296(4)	1.289(4)	1.289(2)	1.291(3)	1.287(2)
N1−C2	1.359(5)	1.354(5)	1.356(4)	1.338(4)	1.344(4)	1.332(4)	1.343(2)	1.347(3)	1.340(2)
N1−C15	1.433(5)	1.413(5)	1.428(4)	1.433(4)	1.422(4)	1.428(4)	1.417(2)	1.421(3)	1.423(2)
N2−C22	1.354(5)	1.339(5)	1.352(4)	1.350(4)	1.340(4)	1.346(4)	1.344(2)	1.340(3)	1.343(2)
N2−C35	1.430(5)	1.429(5)	1.440(4)	1.419(4)	1.426(4)	1.419(4)	1.415(2)	1.420(3)	1.419(2)

[a] Labeling scheme as in Figure 6. [b] The $S_t = {}^3/_2$ molecules reside on site 1, whereas those with $S_t = {}^1/_2$ reside on site 2 at 100 K.

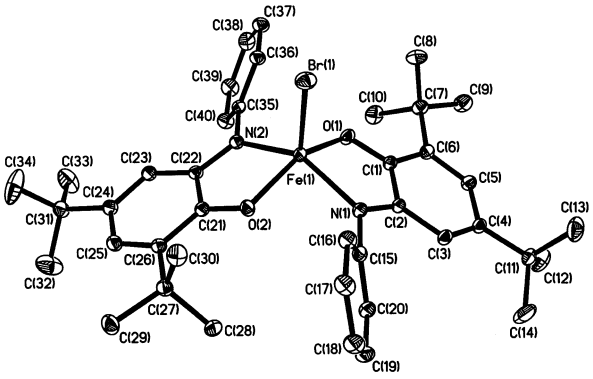

Figure 6. Structure of a neutral $[Fe^{III}Br(L^{ISQ})_2]$ molecule with $S_t = {}^3/_2$ ground state in a crystal of **2b** at 100 K. Hydrogen atoms are omitted.

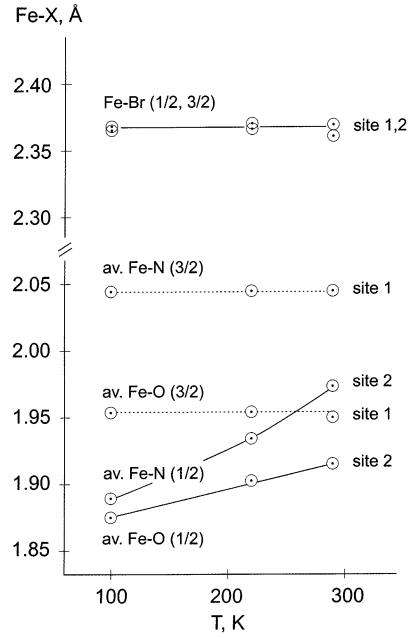

Figure 7. Temperature dependence of apparent Fe−X bond distances in $[Fe^{III}Br(L^{ISQ})_2]$ molecules in a crystal of **2a** as distributed over two crystallographically independent sites 1 and 2.

58:42. These data give an excellent fit of the magnetic data in Figure 1.

The structure of polymorph **2b** has also been determined at 100, 200, and 295 K. This complex also crystallizes in the triclinic space group $P\bar{1}$ but with $Z = 2$. Thus, in **2b**

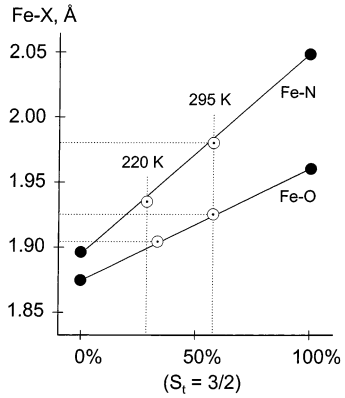

Figure 8. Dependence of the apparent Fe−X bond lengths (X = N,O) on the fraction of $S_t = {}^3/_2$ and $S_t = {}^1/_2$ forms of $[Fe^{III}Br(L^{ISQ})_2]$ molecules residing on site 2 in **2a**. The values for the pure $S_t = {}^3/_2$ form were taken from the structures of **2a** at 100 K on site 1 and **2b** (100, 200, 295 K); those for pure $S_t = {}^1/_2$ were taken from molecules on site 2 in **2a** at 100 K.

there is only one type of neutral molecule $[Fe^{III}(L^{ISQ})_2Br]$ of which the geometric features of the N,O-coordinated ligands are again compatible only with an $(L^{ISQ})^{1\bullet-}$ formulation. The Fe−N and Fe−O bond lengths are long and temperature independent and indicative of the $S_t = {}^3/_2$ form which is experimentally verified by the magnetic susceptibility measurements shown in Figure 1. This study serves as a benchmark for the notion that the bond distances of the pure $S_t = {}^3/_2$ forms (and by conjecture of the pure $S_t = {}^1/_2$ form) of complexes **1**, **2b**, and **3** are temperature independent in the range 100−300 K.

The structure of $[Fe^{III}(L^{ISQ})_2I]$ (**3**) at 100 K unequivocally showed the presence of the pure $S_t = {}^1/_2$ form. The Fe−N and Fe−O bond lengths at 1.885(2) and 1.875(1) Å are very short. Using the same crystal, we have collected new data sets at 220 and 295 K; the results of the structure determination are given in Table 6. As shown in Figure 9, the apparent Fe−O and Fe−N bond distances increase with increasing temperature, and we can estimate the presence of 16% of the $S_t = {}^3/_2$ form and 84% of the $S_t = {}^1/_2$ form at 295 K. Thus, this experiment proves that the temperature dependence of the effective magnetic moment of **3** is due to spin crossover behavior and not exchange coupling as indicated in our original paper.[2] Note that the apical Fe−I distance is again temperature-independent in the range 100−295 K.

Table 6. Selected Bond Distances (Å) of $[Fe^{III}I(L^{ISQ})_2]$ Molecules in a Crystal of **3** as a Function of the Temperature[a]

	100 K	220 K	295 K
I−Fe	2.5912(5)	2.5910(3)	2.5911(6)
Fe−O2	1.869(1)	1.887(1)	1.902(2)
Fe−O1	1.881(1)	1.879(1)	1.899(2)
Fe−N2	1.885(2)	1.894(1)	1.921(2)
Fe−N1	1.885(2)	1.895(1)	1.925(2)
O1−C1	1.313(2)	1.305(2)	1.303(3)
O2−C21	1.306(2)	1.305(2)	1.305(3)
N1−C2	1.358(3)	1.354(2)	1.351(3)
N1−C15	1.436(3)	1.433(2)	1.430(3)
N2−C22	1.356(3)	1.354(2)	1.344(3)
N2−C35	1.425(3)	1.429(2)	1.430(4)

[a] Labeling scheme as in Figure 6 (except that Br is replaced by I).

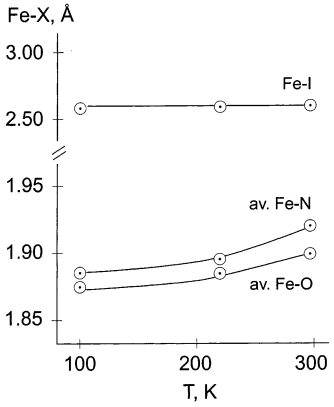

Figure 9. Dependence of the apparent Fe−X bond lengths on the temperature in a crystal of **3**.

Table 7. Selected Bond Distances (Å) in $[Fe^{III}(N_3)(L^{ISQ})_2]$ (**4**) at 100 K and (in Parentheses) at 295 K

Fe−O1	1.879(1) (1.909(1))	O31−C31	1.310(1) (1.303(2))
Fe−O31	1.873(1) (1.910(1))	C31−C32	1.427(1) (1.424(2))
Fe−N7	1.879(1) (1.928(1))	C31−C36	1.429(2) (1.433(2))
Fe−N37	1.887(1) (1.937(1))	C32−C33	1.384(2) (1.369(2))
Fe−N11	1.958(1) (1.948(2))	C33−C34	1.435(2) (1.432(3))
N11−N12	1.221(2) (1.210(3))	C34−C35	1.376(2) (1.363(2))
N12−N13	1.151(2) (1.135(3))	C35−C36	1.421(2) (1.418(2))
O1−C1	1.308(1) (1.300(2))	C36−N37	1.359(1) (1.350(2))
C1−C2	1.431(1) (1.427(2))	N37−C38	1.431(1) (1.433(2))
C1−C6	1.431(1) (1.437(2))		
C2−C3	1.383(2) (1.372(2))		
C3−C4	1.436(2) (1.433(2))		
C4−C5	1.376(1) (1.369(2))		
C5−C6	1.419(1) (1.411(2))		
C6−N7	1.357(1) (1.349(2))		
N7−C8	1.425(1) (1.423(2))		

The structure of **4** has been determined at 100 and 295 K; the results are summarized in Table 7. Crystals of **4** consist at 100 K exclusively of $[Fe^{III}(L^{ISQ})_2(N_3)]$ molecules with an $S_t = {}^1/_2$ ground state. Figure 10 shows the structure of the neutral molecule. The C−O, C−N, and C−C bond lengths clearly indicate the presence of two N,O-coordinated *o*-iminobenzosemiquinonate(1−) π radical anions, and the short Fe−O and Fe−N_{imino} distances at 1.875(1) and 1.883(1) Å, respectively, are typical for the $S_t = {}^1/_2$ form. The azido anion is end-on coordinated in the apical position of the square-pyramidal FeN_3O_2 polyhedron. The Fe−N11−N12 bond angle at 110.5(1)° is small. The Fe−O and Fe−N bond distances increase slightly upon raising the temperature to

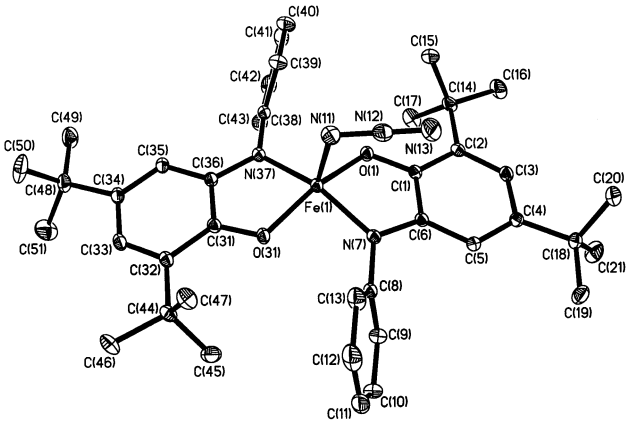

Figure 10. Structure of the neutral molecule $[Fe^{III}(N_3)(L^{ISQ})_2]$ at 100 K in crystals of **4**.

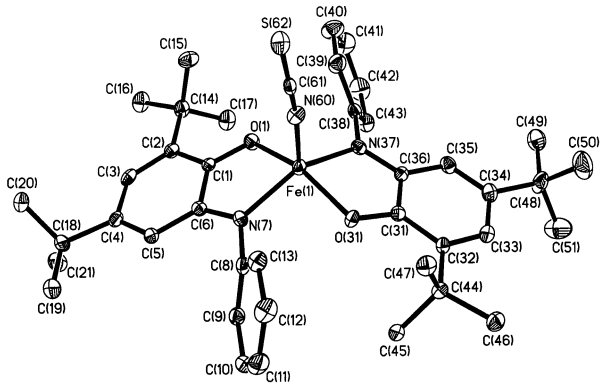

Figure 11. Structure of the neutral molecule $[Fe^{III}(NCS)(L^{ISQ})_2]$ at 100 K in crystals of **5**.

Table 8. Selected Bond Distances (Å) in $[Fe^{III}(NCS)(L^{ISQ})_2]$ at 100 K

Fe−O1	1.939(3)	C3−C4	1.448(7)
Fe−O31	1.945(3)	C4−C5	1.362(7)
Fe−N60	1.952(5)	C5−C6	1.416(7)
Fe−N7	1.997(4)	C6−N7	1.355(6)
Fe−N37	2.019(4)	N7−C8	1.408(6)
O1−C1	1.286(6)	O31−C31	1.286(6)
C1−C2	1.437(7)	C31−C36	1.432(7)
C1−C6	1.444(7)	C31−C33	1.433(7)
C2−C3	1.370(7)	C32−C33	1.363(7)
N60−C61	1.157(7)	C33−C34	1.440(8)
C61−S62	1.617(6)	C34−C35	1.344(8)
		C35−C36	1.443(7)
		C36−N37	1.335(6)
		N37−C38	1.411(6)

295 K, and a ∼20% contribution of the $S_t = {}^3/_2$ form is estimated to be present.

Since solid **5** exists exclusively in its $S_t = {}^3/_2$ form in the temperature range 3−300 K, we have determined its crystal structure at 100 K only. The results are given in Table 8. Crystals of **5**·$CHCl_3$ consist of $[Fe^{III}(NCS)(L^{ISQ})_2]$ neutral molecules with an $S_t = {}^3/_2$ ground state and a molecule of crystallization of chloroform. Figure 11 exhibits the structure of a neutral molecule. The C−O, C−N, and C−C bond lengths indicate once again the presence of two O,N-coordinated *o*-iminobenzosemiquinonate(1−) π radical anions. The corresponding Fe−O and Fe−N bonds of these ligands are significantly longer than those in **4** in excellent accord with the fact that **5** contains high spin ferric ions ($S_{Fe} = {}^5/_2$; $S_t = {}^3/_2$). The thiocyanato ligand is as expected

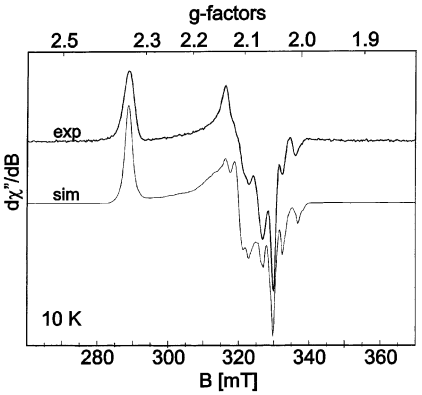

Figure 12. X-band EPR spectrum of **3** (strong line, −) recorded at 10 K in frozen CH_3CN (conditions: microwave frequency, 9.4548 GHz; power, 20 μW; modulation, 1.5 mT/100 kHz). Simulation (thin line, −): $\mathbf{g} = (2.337, 2.109, 2.047)$; $\mathbf{A}(^{127}I) = (3, 15.5, 21.0) \times 10^{-4}$ cm^{-1}; $\mathbf{P} = (-13.3, 7.3, 6.0) \times 10^{-4}$ cm^{-1}; Euler angle $\beta = 26°$ (rotation of the **P** tensor vs **g**, **A**).

N-bound, and the Fe−N60−C61 bond angle is 172.7(4)°. Thus, the Fe−NCS group is nearly linear.

5. EPR Spectrum of 3. Figure 12 displays the X-band EPR spectrum of a frozen acetonitrile solution of **3** at 10 K. It confirms the mononuclear nature of this species and its spin doublet ground state. The spectrum shows well-resolved powder lines in the $g = 2$ region with marked g-anisotropy which arises from a spin−orbit interaction and indicates significant spin density at the ferric ion. Rather surprisingly, the spectrum exhibits a resolved hyperfine splitting at g_{min} with very unusual appearance. It is not possible to simulate the spectrum with any reasonable number of (equal or unequal) nitrogens and protons sensing the spin density. The strong, apparently unsplit "central" hyperfine line at g_{min} cannot be rationalized by using such a model because ^{14}N and ^{1}H are 100% isotopes. A satisfactory simulation was obtained by adopting a hyperfine interaction with a single apical iodide ligand, which is ^{127}I ($I = {}^5/_2$; 100% natural abundance).

The unusual splitting and intensity pattern of these hyperfine lines owe their origin to large electric quadrupole interactions of the iodide ligand which mix and shift the m_I sublevels of the nuclear-spin manifold. This in turn affects the transition probabilities and even induces "forbidden" transitions with virtually $\Delta m_I > 0$, particularly with a nonzero anisotropy factor η. It is important to recall that the influence of quadrupole interactions on EPR hyperfine patterns results from higher-order effects. The reasonable simulation in Figure 12 of the strong perturbations observed requires, therefore, that the electric-field-gradient (EFG) tensor of iodide be oriented "off" from the principal axes systems of the respective **A** tensor.

The major components of the EFG coupling tensor **P** is found virtually in the direction of $\mathbf{g}_{max}$ which is perpendicular to $\mathbf{A}_{max}$ (along $\mathbf{g}_{min}$). The numerical values of the **g**, **A**, and **P** tensors obtained from the simulation are summarized in the caption of Figure 11.

It is noted that a very similar EPR spectrum has recently been reported for the thio analogue of **3**, namely iodo-bis-(*o*-iminothionebenzosemiquinonato)iron(III).[8]

Conclusions

We have shown in this study by a combination of temperature-dependent X-ray crystal structure determinations, magnetochemistry, and Mössbauer and EPR spectroscopy that the neutral complexes $[Fe^{III}X(L^{ISQ})_2]$ in crystals of **2a**, **2b**, **3**, and **4** exist in two different spin states in the range 4−300 K, namely $S_t = {}^3/_2$ and $^1/_2$. Temperature-dependent spin crossover behavior $S_t = {}^1/_2 \leftrightharpoons S_t = {}^3/_2$ is observed in the solid state. Both forms contain two N,O-coordinated *o*-iminobenzosemiquinonate(1−) π radical anions and a halido or pseudohalido ligand in the apical position of a square-planar-pyramidal polyhedron. Interestingly, only the Fe−N and Fe−O bond distances vary with the spin state; the Fe−X bonds are the same in both forms. For the $S_t = {}^1/_2$ forms, the average Fe−N and Fe−O bond lengths are short at 1.885 and 1.875 Å, respectively, but long at 2.047 and 1.951 Å in the corresponding $S_t = {}^3/_2$ forms.

The electronic structures of **1**−**5** are understood in terms of a high spin ferric ion ($S_{Fe} = {}^5/_2$) coupled antiferromagnetically to two π radical anions ($S_{rad} = {}^1/_2$) yielding the observed $S_t = {}^3/_2$ ground state. In contrast, the $S_t = {}^1/_2$ ground state originates from an intermediate spin ferric ion ($S_{Fe} = {}^3/_2$) coupled antiferromagnetically to two π radicals.

Acknowledgment. We thank the Fonds der Chemischen Industrie of Germany for financial support. H.C. is grateful for a fellowship from the Alexander von Humboldt Foundation.

Supporting Information Available: Complete listings of atom coordinates, bond lengths and bond angles, anisotropic thermal parameters, and calculated positional parameters of hydrogen atoms for complexes **2a** (220, 295 K), **2b** (100, 200, 295 K), **3** (220, 295 K), **4** (100, 295 K), and **5** (100 K). Crystallographic data in CIF format. This material is available free of charge via the Internet at http://pubs.acs.org.

IC0301526